PAPER

Aptasensor based optical detection of glycated albumin for diabetes mellitus diagnosis

To cite this article: Shreya Ghosh *et al* 2017 *Nanotechnology* **28** 435505

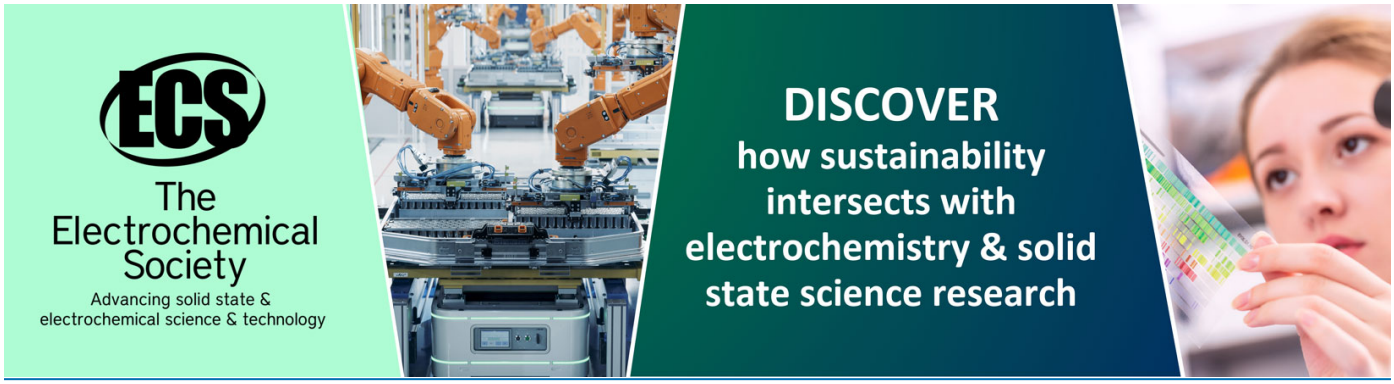

IOP Publishing Nanotechnology
Nanotechnology 28 (2017) 435505 (11pp) https://doi.org/10.1088/1361-6528/aa893a

Aptasensor based optical detection of glycated albumin for diabetes mellitus diagnosis

Shreya Ghosh[1], Debopam Datta[2], Mehar Cheema[1], Mitra Dutta[2,3] and Michael A Stroscio[1,2,3]

[1] Department of Bioengineering, University of Illinois at Chicago, 851 South Morgan Street (SEO 218), Chicago, IL 60607, United States of America
[2] Department of Electrical and Computer Engineering, University of Illinois at Chicago, 851 South Morgan Street, M/C 154, Chicago, IL 60607, United States of America
[3] Department of Physics, University of Illinois at Chicago, 845 W. Taylor St. (M/C 273), Chicago, IL 60607, United States of America

E-mail: sghosh9@uic.edu

Received 7 July 2017
Accepted for publication 30 August 2017
Published 4 October 2017

Abstract

Glycated albumin (GA) has been reported as an important biomarker for diabetes mellitus. This study investigates an optical sensor comprised of deoxyribonucleic acid (DNA) aptamer, semiconductor quantum dot and gold (Au) nanoparticle for the detection of GA. The system functions as a 'turn on' sensor because an increase in photoluminescence intensity is observed upon the addition of GA to the sensor. This is possibly because of the structure of the DNA aptamer, which folds to form a large hairpin loop before the addition of the analyte and is assumed to open up after the addition of target to the sensor in order to bind to GA. This pushes the quantum dot and the Au nanoparticle away causing an increase in photoluminescence. A linear increase in photoluminescence intensity and quenching efficiency of the sensor is observed as the GA concentration is varied between 0–14 500 nM. Time based photoluminescence studies with the sensor show the decrease in binding rate of the aptamer to the target within a specific time period. The sensor was found to have a higher selectivity towards GA than other control proteins. Further investigation of this simple sensor with greater number of clinical samples can open up avenues for an efficient diagnosis and monitoring of diabetes mellitus when used in conjunction with the traditional method of glucose level monitoring.

Keywords: aptasensor, glycated albumin sensor, DNA aptamer, FRET, glycated albumin, molecular beacon, optical sensor

(Some figures may appear in colour only in the online journal)

1. Introduction

Diabetes has been termed as one of the leading causes of global mortality. According to the World Health Organization, in 2014, approximately 422 million adults were found to have diabetes in comparison to 108 million people in 1980 [1]. Diabetes is a chronic state where the pancreas is unable to produce enough insulin and hence results in elevated glucose levels in bloodstream [2]. Such a condition is referred to as hyperglycemia [3]. It causes elevated concentrations of glycated proteins such as albumin and hemoglobin in the human system [4, 5]. Diabetic nephropathy is a type of kidney failure caused by the incidence of diabetes.

The most common clinical method adopted for monitoring diabetes, so far, is the combined measurement of blood glucose and glycated hemoglobin (HbA1c) levels. However, HbA1c levels can often be unreliable for patients with disorders such as hemolytic anemia, thalassemia etc. Fructosamine is also utilized for tracking glycemic index. However, fructosamine concentrations are highly dependent on

concentrations of proteins, bilirubin, hemoglobin and various low molecular weight substances in the human system [5, 6]. The half-lives for some of these proteins have not been estimated yet. Hence, fructosamine concentrations are often inaccurate. Therefore, glycated albumin (GA) has been determined to be a much more accurate marker for diabetes mellitus [5] especially for patients undergoing hemodialysis [7] or having hematologic disorders [8].

GA has come to the forefront as a tool for both the control and diagnosis for diabetic patients. GA begins with human serum albumin (HSA) and is developed into GA through a series of modifications and reactions. GA may be used as a glycemic control tool based on the extent of glycation depending on time allowed for glycation and amount of glucose available for reaction with HSA [9]. GA can also be used as an accurate marker in such pathologies including hemolytic anemia and deficiency anemia of diabetic patients [10]. While many markers exist that are currently used for diabetes management and predictive measures, GA provides many advantages including earlier detection and prolonged circulation in the body. Measurement of glucose levels in the blood is the standard management method for diabetes management and detection. GA provides an alternative method to simple blood glucose detection and may offer an alternative diagnostic and prognostic marker for many diabetic patients. Using GA as a marker over long controlled periods of time (2–3 months) is made possible through the extended life span of hemoglobin levels in red blood cells [9]. Advantages of GA detection over typical blood glucose level measurement is also the ability to detect worsening glycemic control at an earlier stage compared to HbA1c detection [11]. It has also been seen that prolonged elevation of GA levels can lead to irreversible damage that is associated with diabetes mellitus, including neuropathy and coronary artery disease [12]. Therefore, to achieve a better diagnosis and management of diabetes, detection of glucose levels can be assisted by GA detection.

The process of glycation of HSA is divided into several stages, first of which combines reduction of sugar (glucose) with primary amine groups to form a reversible Schiff base, which through further modification develops an Amadori product [13–17]. Many sugar molecules may be used to modify albumin, including galactose and fructose [18]. Following the Amadori product formation, the next stage involves the oxidation of glycated proteins that form reactive dicarbonyl compounds [9]. These reactive compounds further react with lysines and arginines to form AGE compounds, which include methylglyoxal-derived hydroimidazolone isomer 1 (MG-H1) and glyoxal-derived hydroimidazolone isomer 1 (G-H1) that have been seen in previous studies of GA [9]. Through these numerous steps of modification, HSA is glycated and goes through the transition to become GA. The primary functional groups of GA that are affected by glycation are lysine, arginine and cysteine [19]. The functional impact of GA has been shown to stabilize the tertiary and secondary structures and acquire a high life span [20]. The glycation process is often associated with oxidation processes as well, which are referred to as glycoxidation and affect early stages of the glycation process [21]. Previous studies show that higher levels of GA induce oxidative damage to cells [22, 23].

Single stranded deoxyribonucleic acid (DNA) aptamers have been extensively studied by researchers previously for the detection of a wide range of targets such as metals ions including lead [24, 25], mercury [26], potassium [25], as well as biomolecules such as ATP [27] and AMP [28], and proteins such as C-reactive protein (CRP) [29], interferon gamma (IFN-γ) [30], etc. DNA aptamers are defined as oligonucleotides, which contain a single, typically short, sequence of DNA that bind to specific antigens including molecules and ions. Using these short DNA sequences, targeting of specific molecules such as GA is facilitated through the aptamer binding sequences. One approach used frequently with aptamers involves using quantum dots; the resulting complexes are referred to as molecular beacons (MBs) [31]. MBs find a wide variety of applications in DNA binding protein detection [32, 33], metal ions such as potassium [34, 35], and have also been used as nucleic acid hybridization probes extensively [36]. Quantum dot technology is facilitated by aptamer and molecule binding via fluorescence resonant energy transfer (FRET). Dyes, quenchers, and metal nanoparticles can all serve as possible acceptors via FRET [37]. The mechanism of FRET transfer may be facilitated through quantum dot-gold nanoparticle interactions. When a quantum dot is brought into proximity of an Au nanoparticle once the aptamer binds the target molecule, the quantum dot fluorescence is then quenched via energy transference to the gold nanoparticle instead of the energy being emitted as a photon [25]. Since the absorption spectrum of gold nanoparticles is quite broad, they are quite effective as a quenching mechanism for quantum dot technology. Previous studies have established the quenching efficiency is proportional to $1/d^6$ for distances smaller than d_0 and $1/d^4$ for distances larger than d_0, defined as d being the distance of the emitter from the quencher and d_0 is the characteristic distance where quenching and light emission are seen to be equal approximately 5 nm [25]. Nanosurface energy transfer is another phenomenon based on FRET for the case where a point-like object interacts with a local surface to promote quenching of light emission; in this case the change in light emission scales as $1/d^4$, and demonstrates the wide range of utility of FRET-based phenomena [25]. Gold nanoparticles have the capability to work through both FRET and NSET technology which demonstrates why they are typically used as quenchers in quantum dot systems.

Previous works show that GA can be detected using enzymatic methods [5, 38–40], affinity chromatography [6, 41–43], immunochemistry [44, 45]. While enzymatic sensors suffer various drawbacks such as high pH and temperature sensitivity [46], higher chances of denaturation and are therefore highly difficult to use enzymes in an *in vitro* environment [47, 48], the other methods require longer processing times and exhibit poor precision [38]. Optical sensing of GA has been determined to be one of the most promising methods of detection since they do not require significant sample preparation and are relatively faster and cheaper [49]. Raman spectroscopy has been used to detect GA [50]. However, the limit of detection (LD) of the method was

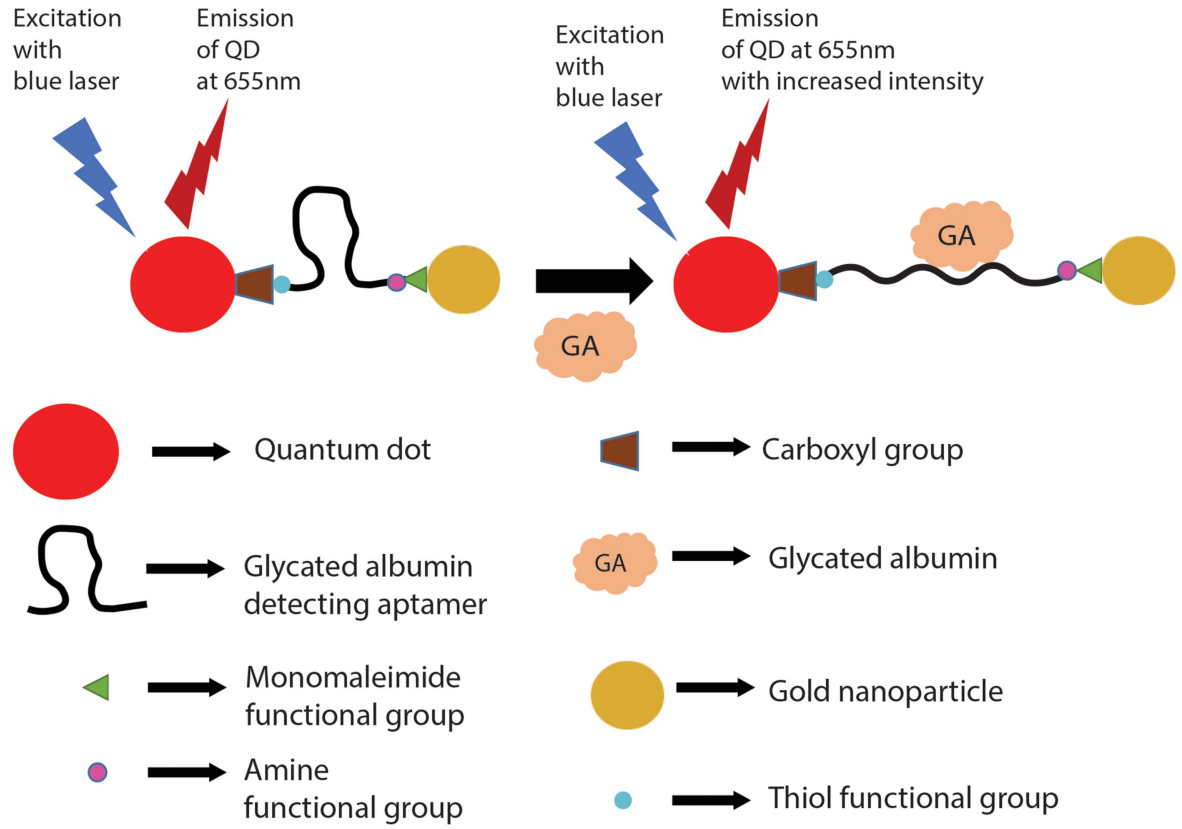

Figure 1. Molecular beacon for the detection of glycated albumin. This figure illustrates the principle behind the detection of glycated albumin using fluorescence resonant energy transfer. An increase in PL intensity is observed after the addition of the addition of the target in the sensor.

higher than that of the sensor proposed in our study. Other GA detection platforms includes fructosamine 6-kinase based electrochemical sensing [51, 52], electrochemiluminescence sensing [53], surface plasmon resonance sensing [54] and aptamer based sensing [55].

In this study, we have synthesized a MB, where the DNA aptamer is attached to the quantum dot on one end and Au nanoparticle quencher to the other end for the detection of GA (figure 1). Such a platform can be potentially used for monitoring diabetes.

2. Methods

2.1. Aptamer structure and modification

The GA binding aptamer used in this study was purchased from Biosearch Technologies (Petaluma, CA). It consists of 23 base pairs and has been modified on both ends with an amine group on the 5′ and a Thiol group on the 3′ (5′Amino C6/TGCGGTTGTAGTACTCGTGGCCG/Thiol C6 SS 3′). The aptamer was dissolved into Tris Ethylenediamine Tetraethyl Acetate buffer to obtain 100 μM aptamer solution.

2.2. Materials

GA, non-glycated HSA, transferrin and Immunoglobulin-G (IgG) were purchased from Sigma Aldrich (St. Louis, MO). CRP was obtained from EMD-Millipore (Temecula, CA) while recombinant human IFN-γ was purchased from BioLegend (San Diego, CA). Human serum (HS) was obtained from AB plasma of human male (Sigma Aldrich Inc., St. Louis, MO.) 1-ethyl-3-(3-dimethylaminopropyl)-carbodiimide (EDC) and tris(2-carboxyethyl) phosphine (TCEP) are obtained from Pierce Biotechnology (Rockford, IL). 20 nm carboxyl coated CdSe/ZnS QDs e-flour ITK 655NC with an average radius of 20 nm were purchased from Life Technologies (Carlsbad, CA). Monomaleimide functionalized nanogold (Au) particles having a diameter of 1.4 nm was obtained from Nanoprobes (Yaphank, NY). Nanosep molecular weight cutoff (MWCO) filters of 10 and 100 k pore sizes were purchased from Pall Lifesciences (Ann Arbor, MI).

2.3. Synthesis of MB

9 μl of TCEP was added to 20 μl of the 100 μM GA aptamer and incubated for 30 min at room temperature. This process facilitates the reduction of the dithiol groups in the aptamer. 100 μl of deionized water was added to one vial of Au nanoparticles. The entire volume of Au nanoparticle solution was added to the thiol activated GA aptamer-TCEP solution in a 3:1 ratio. The final solution was further incubated for 2 h at room temperature. After 2 h, the excess gold nanoparticles were filtered out by centrifuging the solution twice at 7000 rpm for 15 min each using a 10 k MWCO

filter. 13 μl of quantum dots were mixed with 87 μl of 10 mM borate buffer (pH 7.4). This quantum dot solution was further added to the GA aptamer/Au nanoparticle solution in the presence of 23 μl of 4 μg μl^{-1} EDC/Sulfo NHS solution. This solution was then allowed to stir gently for 2 h at room temperature. Subsequently, the samples are centrifuged at 7000 rpm for 5 min using a 100 k MWCO filter in 50 mM borate buffer (pH 8.3). This process is repeated 10 times to eliminate unbound aptamers and EDC from the sensor solution.

2.4. Analytical selection and prediction of secondary structure of GA aptamer

The secondary structure of the GA binding aptamer was determined using M-fold web server [56–58]. The parameters that were used to determine the structure was temperature and ionic concentration. Two temperature conditions were considered: (1) 25 °C, which is the room temperature and (2) 37 °C, which is the temperature under physiological conditions. For each of these temperatures, there were two different ionic condition considered: (1) 1.37 mM Na^+ and (2) 10 mM Na^+.

2.5. Optical detection of GA

The GA samples for the optical detection test were prepared by adding 0.005, 0.1, 1, 5, 10, 40 and 95 mg GA to 1 ml of 0.01 XPBS each. 5 μl of these GA samples were then added to 750 μl of sensor solution in a cuvette while keeping the cuvette undisturbed in the holder. The DNA aptamer in the sensor is allowed to bind to GA for 2 h before the photoluminescence intensity is recorded. The same conditions were repeated during the optical detection experiments with the control proteins and the clinical samples. The control proteins used for these experiments are non-glycated HSA, CRP, transferrin, IgG and IFN-γ. Their stock solutions were also made in 0.01 XPBS.

HS was used for preparation of clinical samples. 100 μl of HS solution is spiked with 0.1 mg named sample-S2 (see Results and discussion) and 0.95 mg of GA named sample S3 to simulate real life clinical sample and unspiked HS solution named sample S1 was used as the control counterpart for the clinical samples. The sample volume is used as 5 μl for the clinical samples to maintain uniformity with the pure samples.

2.6. Instruments

The photoluminescence measurements of the sensor were conducted using a USB4000 Ocean Optics (Dunedin, FL, USA) spectrophotometer with a continuous 375 nm LED excitation. The centrifuge used was Fisher Scientific Accuspin micro (Fisher Scientific, USA).

3. Results and discussion

3.1. Analytical selection and prediction of secondary structure of GA binding aptamer

The GA binding aptamer was chosen based on a previous study by Apiwat *et al* [55], where the DNA aptamer showed sensitivity towards GA. Apart from this, the choice was also based on the possibility of FRET between the quantum dot and the Au nanoparticle quencher. Since, the length of a single DNA base is 0.34 nm, the 23 base GA binding aptamer has a length of 7.82 nm. The presence of the Amino C6 modifier along with the Thiol C6 SS modifier will add another 1.2 nm approximately to the length of the DNA aptamer because of their combined 12 C–C bonds. This will result in an approximate distance of 9 nm between the quantum dot and the Au nanoparticle quencher.

The M-fold webserver software predicted the secondary structures of the GA aptamer under the conditions mentioned in section 2.3. The aptamer was found to have a similar structure for all the conditions and is characterized by the formation of a hairpin loop at G^5 and C^{21}. This has been clearly shown in figures 2(a)–(d). The aptamer structures shown in figures 2(a)–(d) have been chosen in such a way that they have the lowest ΔG. Table 1 represents the ΔG values of the aptamer under all the condition mentioned in section 2.3.

Based on the structure of the aptamer at 1.37 mM Na^+ concentration at a folding temperature of 25 °C (figure 2(a)), it can be concluded that the GA binding aptamer remains in a hairpin loop structure before the addition of any analyte. This phenomenon results in bringing the quantum dot and the Au nanoparticle quencher closer to each other to an approximate distance of 2 nm (figure 3). As discussed later in the paper, an increase in photoluminescence is observed on the addition of the analyte, therefore it is assumed that the hairpin loop plays a significant role the binding of GA to the aptamer by opening up the hairpin loop and putting the quantum dot and Au nanoparticle quencher farther apart to a maximum distance of 9 nm approximately (figure 3).

3.2. Optical detection of GA

3.2.1. Sensitivity and specificity of the aptasensor towards GA. The sensitivity of the aptamer based sensor towards GA was evaluated by adding the target progressively in concentrations ranging between 0 and 14 500 nM in the assay. As shown in figure 4(a), the photoluminescence intensity increases with an increase in the concentration of GA in the liquid sensor assay. This behavior is repeated when other sensor samples are tested with the same procedure and exhibits a steady linear increase in photoluminescence intensity over the same concentration range of GA (figure 4(b)). This phenomenon can be attributed to the conformational change of the aptamer. In section 3.1, it has been mentioned that the DNA aptamer acquires a large hairpin loop like structure, which brings the quantum dot and the Au nanoparticle quencher closer. On the addition of GA, it is assumed that the aptamer unfolds

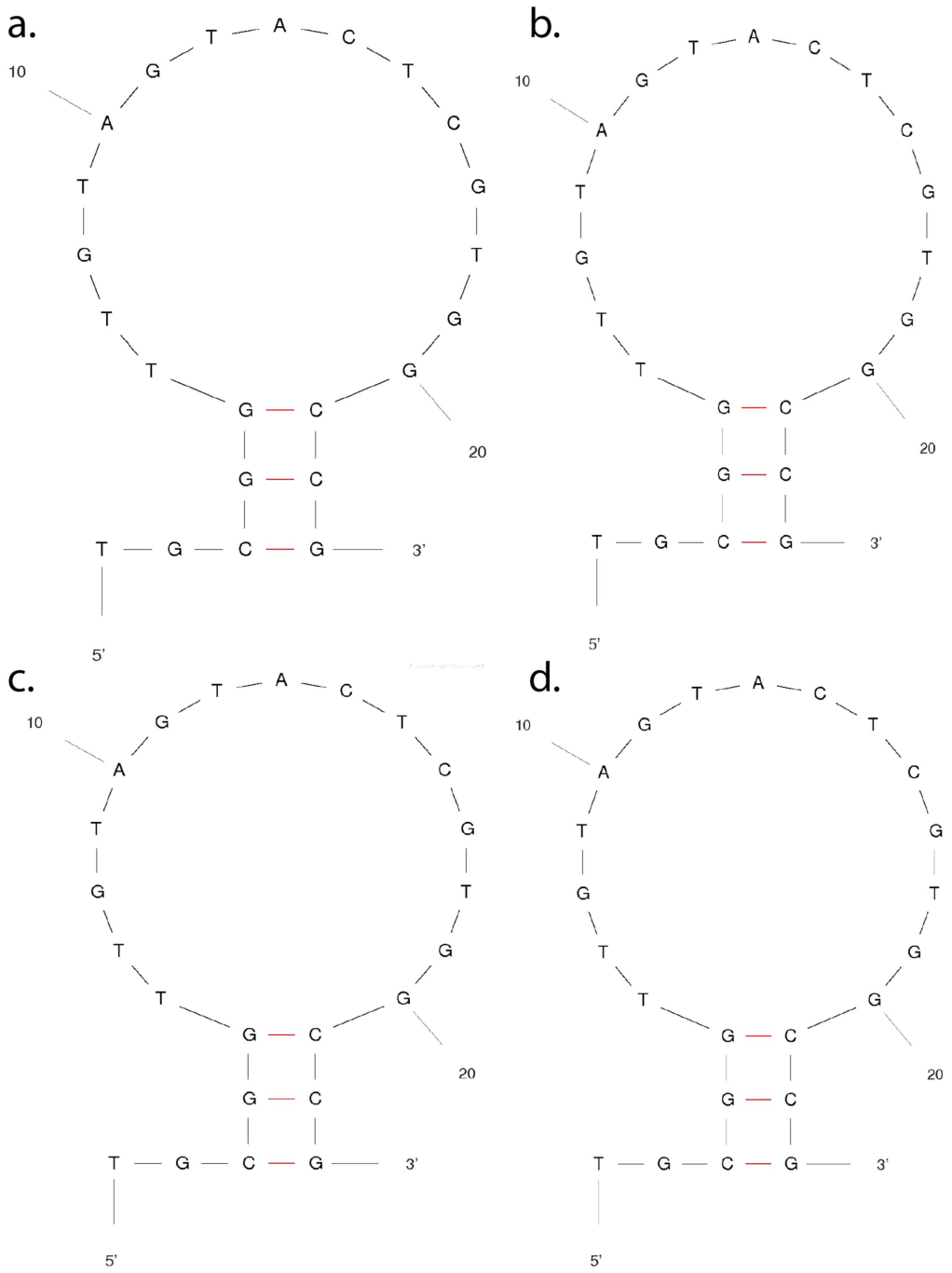

Figure 2. Secondary structure of the GA binding aptamer at (a) 1.37 mM Na^+ concentration and 25 °C temperature, (b) 10 mM Na^+ concentration and 25 °C temperature (c) 1.37 mM Na^+ concentration and 37 °C temperature and (d) 10 mM Na^+ concentration and 37 °C temperature.

Table 1. Variation of Gibb's free energy values when the GA binding aptamer folds under different ionic and temperature conditions.

Sl. no.	Parameter	ΔG (kcal mol^{-1})
1.	1.37 mM Na^+ concentration and 25 °C temperature	−0.18
2.	10 mM Na^+ concentration and 25 °C temperature	−0.72
3.	1.37 mM Na^+ concentration and 37 °C temperature	0.95
4.	10 mM Na^+ concentration and 37 °C temperature	0.37

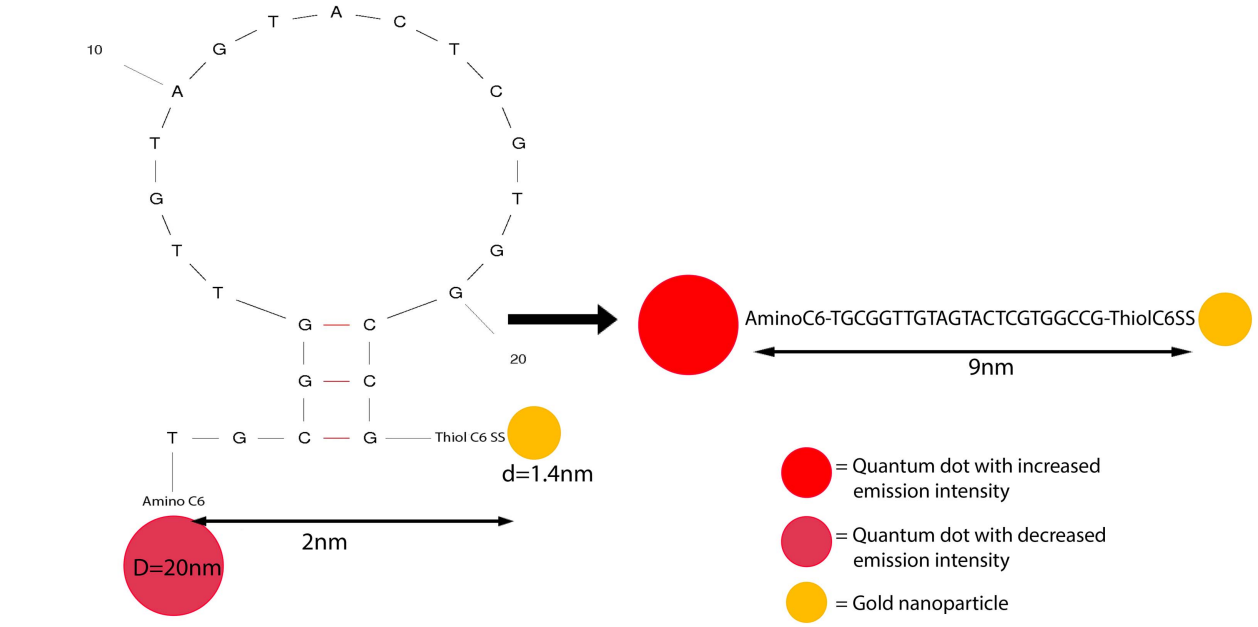

Figure 3. Schematic showing the change in the approximate distances between the quantum dot and the gold nanoparticle quencher before and after the addition of GA. The folded structure of the DNA aptamer before the addition of the analyte was predicted by M-fold webserver software.

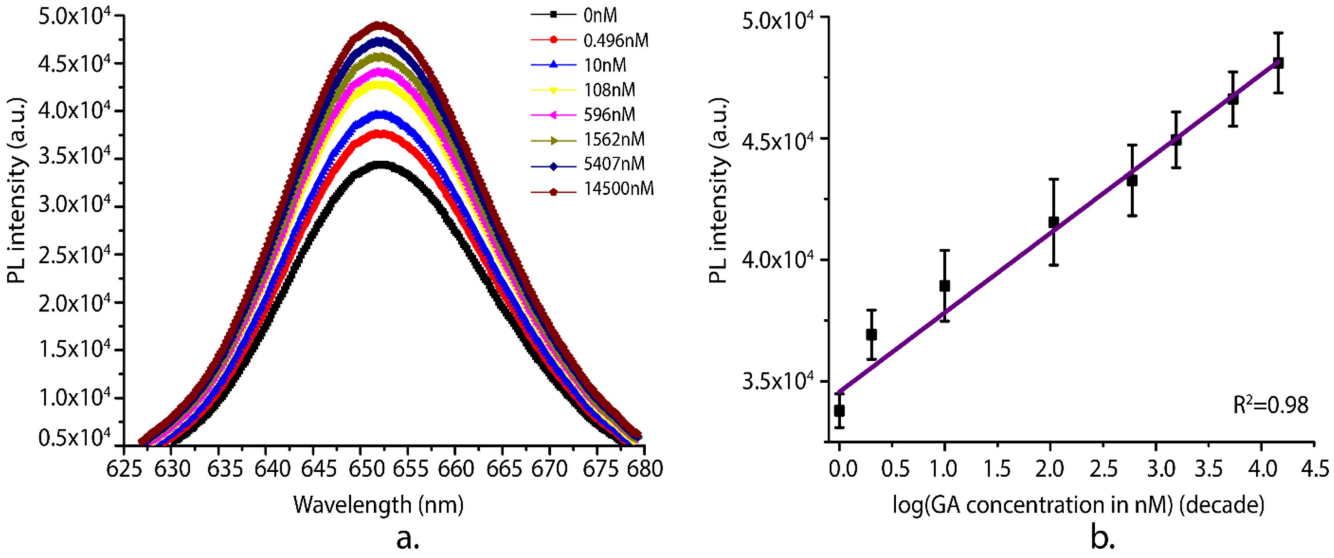

Figure 4. (a) Photoluminescence intensity of as a result of adding varied concentrations GA to 750 μl of the DNA aptamer based sensor solution. (b) Linear increase in the averaged photoluminescence intensity over the logarithm of the GA concentrations added to the sensor. The photoluminescence intensity was collected from six different sensor samples ($n = 6$) and the GA concentrations stated are its concentration in the assay.

from the hairpin loop like structure in order to bind to GA. This pushes the quantum dot and the Au nanoparticle quencher further apart, thus, causing an increase in the photoluminescence intensity. GA consists of a large number of arginine and lysine residues [59]. It has been previously studied that arginine and lysine exhibits a strong interaction with guanine while arginine also interacts with adenine and thymine [60]. The chosen DNA aptamer has 9 guanine bases and 7 thymine bases out of the entire 23 base structure and these bases comprise a major part of the hairpin loop as well as the external loop. Therefore, there is a high possibility that the hairpin loop plays a crucial role in the GA-aptamer complex formation.

The quenching efficiency (figure 5(a)) of the sensor was calculated by using the equation (1), where QE is the quenching efficiency, I is the photoluminescence intensity after the addition of target analyte at a specific concentration and I_0 is the photoluminescence intensity before the addition

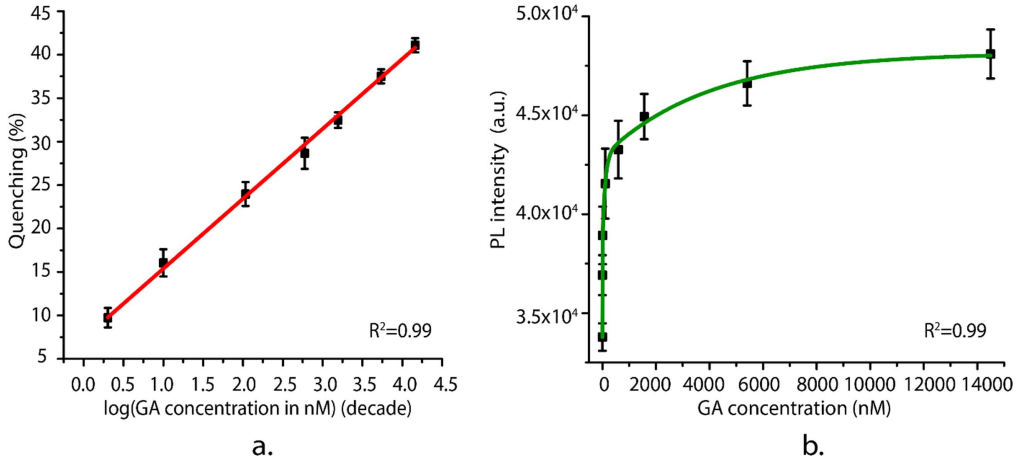

Figure 5. (a) Quenching efficiency demonstrated by the sensor on the addition of progressive addition of GA concentrations, the logarithm of which has been shown here. This represents the sensitivity of the sensor samples to the target GA. (b) Relationship between PL intensity and concentration of GA in nM. Experiments have been conducted with six different sensor samples in both cases ($n = 6$).

Table 2. Comparison of the limit of detection of several GA detecting platforms with that of the proposed aptasensor in this study.

Sl. no.	Type of sensor	Limit of detection	Reference
1.	Enzymatic assay based electrochemiluminescence sensor	0.1 μM (6.6 μg ml^{-1})	[53]
2.	Enzymatic assay based sensor	0.36 mg ml^{-1}	[62]
3.	Electrochemical aptasensor	3 μg ml^{-1}	[63]
4.	Raman spectroscopy based sensor	13.7 μM	[50]
5.	Graphene based optical aptasensor	50 μg ml^{-1}	[55]
6.	Enzymatic assay based colorimetric sensor	0.47 mg ml^{-1}	[61]
7.	HPLC based boronate immunoassay	>10.9 μM	[45]
8.	Hydrazine based colorimetric sensor	0.7 μM	[64]
9.	Affinity chromatography based immunoturbimetric sensor	0.81 mg l^{-1}	[6]
10.	Optical aptasensor	1.08 nM (0.067 μg ml^{-1})	This work

of target.

$$\mathrm{QE} = \left(\frac{I - I_0}{I_0}\right) \times 100. \quad (1)$$

As can be seen in figure 5(a), the sensor exhibited quenching efficiencies of 9.74% ± 1.12% and 41.09% ± 0.81% when the concentration of GA in the assay was 0.5 nM and 14 500 nM respectively. The concentration of GA (in nM) was converted to the corresponding logarithm value to show the linear behavior of the sensor ($R^2 = 0.99$). Figure 5(b) represents the behavior of the sensor when the original PL intensities are plotted w.r.t. the concentration of GA in nM.

The LD was calculated using equation (2), where SD_0 is standard deviation for blank sample, sensitivity is the slope of the quenching curve (shown in figure 5(a)). LD is the logarithm value of the GA concentration expressed in nM.

$$\mathrm{LD} = \frac{3 \times \mathrm{SD}_0}{\mathrm{Sensitivity}}. \quad (2)$$

It was found that the average LD for the sensor was 1.008 nM. Considering the molecular weight of GA is 66.5 kDa, the LD (1.008 nM or 0.067 μg ml^{-1}) of this sensor is significantly lower than those reported in previous studies such as 0.47 mg ml^{-1} from the enzymatic assay [61] and 50 μg ml^{-1} from the graphene based aptasensor [55]. Table 2 compares the LD of this aptasensor with various other GA sensing platforms. It clearly shows that the LD of the aptasensor proposed in this paper is superior to previously published platforms. Also, the concentration of GA in HS was found to be 3–105.3 μM (0.2–7.0 mg ml^{-1}) [55, 61]. Therefore, the aptasensor can potentially detect the presence of GA easily in diabetic serum.

In order to study the DNA-protein reaction behavior, a time based optical study was conducted. In this, once 5 μl of GA of a certain concentration was added, PL intensities were recorded after specific intervals of time (0–120 min). Figure 6(a) shows that the PL intensities increases almost linearly with the progression of time and concentration of GA. The time based quenching values (QE_T) represented figure 6(b) have been calculated as the normalized difference

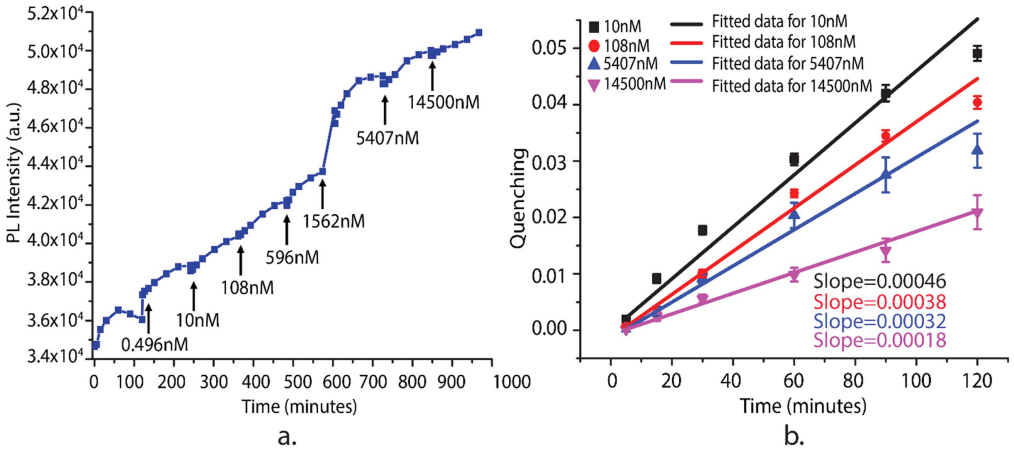

Figure 6. Time based change in (a) PL intensity of the aptasensor on successive addition of GA concentrations ranging between 0.496 and 14 500 nM. (b) Quenching values of the sensor on addition of different concentrations of GA. Experiments have been conducted with six samples ($n = 6$).

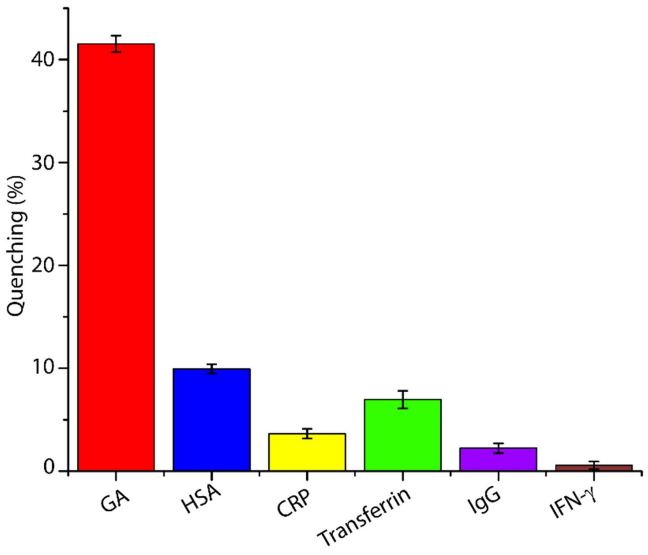

Figure 7. Response of the aptasensor towards control proteins. This graph compares the specificity of the sensor to GA and other control proteins, some of which have a high structural similarity with GA such as HSA. Experiments have been conducted in triplicates ($n = 3$).

between PL and PL_0 by using equation (3), where PL represents the PL intensity recorded after a specific period of time following the addition of target while PL_0 is the PL intensity before the addition of target.

$$QE_T = \frac{(PL - PL_0)}{PL_0}. \quad (3)$$

It was observed that the slopes of the quenching curves decrease with the increase in concentration of the target GA. This indicates that the reaction rate decreases with increase in concentration of GA. This behavior can be attributed to the fact that the DNA binding sites are getting occupied as more GA is introduced in the sensor.

The specificity test of the aptasensor was conducted by comparing its response to GA and some control proteins, HSA being the most important out of them. As can be seen in figure 7, GA exhibited the maximum quenching of 41.09% ± 0.81% followed by HSA (9.93% ± 0.45%), Transferrin (6.97% ± 0.85%) and CRP (3.65% ± 0.45%). The cross reactivity of the aptamer with HSA is because HSA has a very similar structure to that GA. However, the control solutions for HSA, Transferrin, CRP and IgG were prepared in such a way that their concentration in assay was 15 μM except IFN-γ which was kept at a concentration of 142 nM. Since, GA shows a quenching efficiency significantly higher than that exhibited by the control proteins at the same concentration, it can be said that the aptamer chosen is fairly specific to GA.

3.2.2. Aptasensor response to clinical samples. Experiments with clinical samples were performed to evaluate the viability of this sensor to detect GA in human blood using glucose meters or continuous glucose monitoring method. The HS which contains most of the proteins, electrolytes, antibody and antigens except the fibrinogen, white blood cells and red blood cells which consists of 55% of the total volume of blood. Hence using HS as the background matrix for the clinical sample can be used to hypothesize the effect of real blood sample. Total protein content of the serum is 4–9 gm dL^{-1} specified by the manufacturer [65], hence the percentage quenching of 10% for sample S1 shown in figure 8(a) is assumed to be due to presence of proteins in the serum. Percentage quenching exhibited by the sample S2 is lower compared to that of sample S1 hence, pure HS sample can produce false positives for detection of 100 nM of GA. Whereas sample S3 shows a statistically significant higher quenching efficiency compared to control sample, hence sample S1 does not behave as a false positive target for detection of 1 μM GA concentration. The possible reason

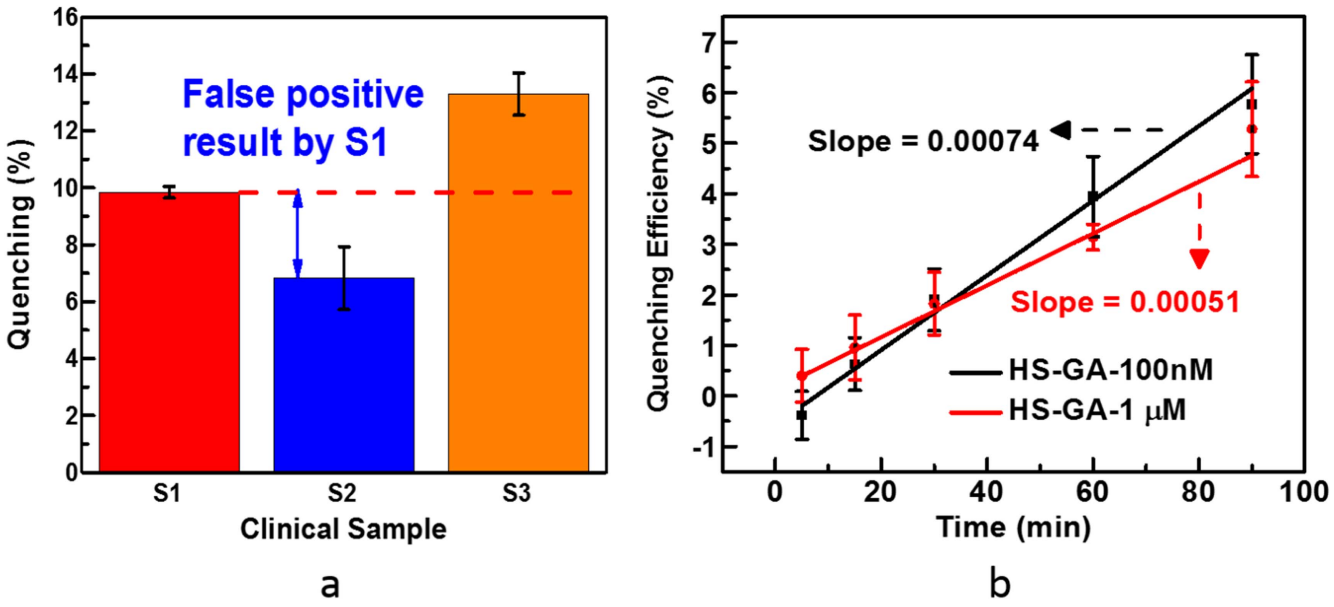

Figure 8. The percentage quenching is being presented in (a) which shows approximately 10% percentage quenching which can be co-related to quenching obtained for HSA in figure 7. Sample S1 behaves as a false positive for the concentration of 100 nM which almost 30 times higher compared to limit of detection obtained from characteristics curve. (b) shows the change in quenching efficiency with time after addition of 5 μl of samples S2 and S3 to the sensor sample.

behind high cross-reactivity towards HS is due to presence of different electrolytes and high concentration of albumin.

4. Conclusion

In this study, we have developed and characterized a simple DNA aptamer based sensor for the detection of GA. It functions on the principle of FRET rendering an increase in photoluminescence with the increase in GA concentration. This research demonstrates the capacity of the aptamer-based sensor to detect pure GA samples over a wide concentration range from 1.008–14 500 nM, where its LD is 1.008 nM and is specific to the target. Although, the sample demonstrates a certain range of cross reactivity in the clinical samples, it can still be used in diabetes diagnosis and monitoring more effectively if used in conjunction with the traditional method of glucose monitoring. This is because the photoluminescence signal will be higher for GA than any other protein at the same concentration level.

Acknowledgments

This work was supported in part, by the Army Research Office (ARO) through the MURI Grant No. W911NF-11-1-0024.

References

[1] WHO 2016 *Global Report on Diabetes* (Geneva: World Health Organization) (http://www.who.int/diabetes/global-report/en)
[2] Anon 2015 About diabetes *Int. Diabetes Fed.* (http://www.idf.org/about-diabetes)
[3] Anon Hyperglycemia (High Blood Glucose) Am. Diabetes Assoc. (http://www.diabetes.org/living-with-diabetes/treatment-and-care/blood-glucose-control/hyperglycemia.html)
[4] Bunn H F, Gabbay K H and Gallop P M 1978 The glycosylation of hemoglobin: relevance to diabetes mellitus *Science* **200** 21–7
[5] Kouzuma T, Usami T, Yamakoshi M, Takahashi M and Imamura S 2002 An enzymatic method for the measurement of glycated albumin in biological samples *Clin. Chim. Acta* **324** 61–71
[6] Reed P, Bhatnagar D, Dhar H and Winocour P H 1986 Precise measurement of glycated serum albumin by column affinity chromatography and immunoturbidimetry *Clin. Chim. Acta* **161** 191–9
[7] Inaba M, Okuno S, Kumeda Y, Yamada S, Imanishi Y, Tabata T, Okamura M, Okada S, Yamakawa T and Ishimura E 2007 Glycated albumin is a better glycemic indicator than glycated hemoglobin values in hemodialysis patients with diabetes: effect of anemia and erythropoietin injection *J. Am. Soc. Nephrol.* **18** 896–903
[8] Koga M 2014 Glycated albumin; clinical usefulness *Clin. Chim. Acta* **433** 96–104
[9] Anguizola J, Matsuda R, Barnaby O S, Hoy K S, Wa C, DeBolt E, Koke M and Hage D S 2013 Review: glycation of human serum albumin *Clin. Chim. Acta* **425** 64–76
[10] Furusyo N and Hayashi J 2013 Glycated albumin and diabetes mellitus *Biochim. Biophys. Acta (BBA)-Gen. Subj.* **1830** 5509–14
[11] Koga M and Kasayama S 2010 Clinical impact of glycated albumin as another glycemic control marker *Endocr. J.* **57** 751–62
[12] Cohen M P 2003 Intervention strategies to prevent pathogenetic effects of glycated albumin *Arch. Biochem. Biophys.* **419** 25–30
[13] Maillard L C 1912 Action des acidesamines sur les sucres: formation des melanoidines par voie methodique *C. R. Acad. Sci.* **154** 66–8
[14] Nursten H E 2005 *The Maillard Reaction: Chemistry, Biochemistry, and Implications* (Cambridge: Royal Society of Chemistry)

[15] Lapolla A, Fedele D, Reitano R, Bonfante L, Guizzo M, Seraglia R, Tubaro M and Traldi P 2005 Mass spectrometric study of *in vivo* production of advanced glycation end products/peptides *J. Mass Spectrom.* **40** 969–72
[16] Lapolla A, Fedele D, Seraglia R and Traldi P 2006 The role of mass spectrometry in the study of non-enzymatic protein glycation in diabetes: an update *Mass Spectrom. Rev.* **25** 775–97
[17] Zhang Q, Ames J M, Smith R D, Baynes J W and Metz T O 2008 A perspective on the Maillard reaction and the analysis of protein glycation by mass spectrometry: probing the pathogenesis of chronic disease *J. Proteome Res.* **8** 754–69
[18] Ledesma-Osuna A I, Ramos-Clamont G and Vázquez-Moreno L 2008 Characterization of bovine serum albumin glycated with glucose, galactose and lactose *Acta Biochim. Pol.* **55** 491–7
[19] Rondeau P and Bourdon E 2011 The glycation of albumin: structural and functional impacts *Biochimie* **93** 645–58
[20] Kouzuma T, Uemastu Y, Usami T and Imamura S 2004 Study of glycated amino acid elimination reaction for an improved enzymatic glycated albumin measurement method *Clin. Chim. Acta* **346** 135–43
[21] Lyons T J 1993 Glycation and oxidation: a role in the pathogenesis of atherosclerosis *Am. J. Cardiol.* **71** B26–31
[22] Chesne S, Rondeau P, Armenta S and Bourdon E 2006 Effects of oxidative modifications induced by the glycation of bovine serum albumin on its structure and on cultured adipose cells *Biochimie* **88** 1467–77
[23] Ranjan Singh N, Rondeau P, Hoareau L and Bourdon E 2007 Identification of preferential protein targets for carbonylation in human mature adipocytes treated with native or glycated albumin *Free Radic. Res.* **41** 1078–88
[24] Brenneman K L, Poduri S, Stroscio M A and Dutta M 2013 Optical detection of lead (II) ions using DNA-based nanosensor *IEEE Sens. J.* **13** 1783–6
[25] Meshik X, Xu K, Dutta M and Stroscio M A 2014 Optical detection of lead and potassium ions using a quantum-dot-based aptamer nanosensor *IEEE Trans. Nanobiosci.* **13** 161–4
[26] Brenneman K L, Sen B, Stroscio M A and Dutta M 2010 Aptamer-based optical bionano sensor for mercury (II) ions *Nanotechnology Materials and Devices Conf. (NMDC), 2010 IEEE* (IEEE) pp 221–4
[27] Mukherjee S, Meshik X, Choi M, Farid S, Datta D, Lan Y, Poduri S, Sarkar K, Baterdene U and Huang C-E 2015 A graphene and aptamer based liquid gated FET-like electrochemical biosensor to detect adenosine triphosphate *IEEE Trans. Nanobiosci.* **14** 967–72
[28] Datta D, Meshik X, Mukherjee S, Sarkar K, Choi M S, Mazouchi M, Farid S, Wang Y Y, Burke P and Dutta M 2017 Sub-millimolar detection of adenosine monophosphate using graphene-based electrochemical aptasensor *IEEE Trans. Nanotechnol.* **16** 196–202
[29] Wu B, Jiang R, Wang Q, Huang J, Yang X, Wang K, Li W, Chen N and Li Q 2016 Detection of C-reactive protein using nanoparticle-enhanced surface plasmon resonance using an aptamer-antibody sandwich assay *Chem. Commun.* **52** 3568–71
[30] Farid S, Meshik X, Choi M, Mukherjee S, Lan Y, Parikh D, Poduri S, Baterdene U, Huang C-E and Wang Y Y 2015 Detection of Interferon gamma using graphene and aptamer based FET-like electrochemical biosensor *Biosens. Bioelectron.* **71** 294–9
[31] Leung C-H, Chan D S-H, He H-Z, Cheng Z, Yang H and Ma D-L 2012 Luminescent detection of DNA-binding proteins *Nucleic Acids Res.* **40** 941–55
[32] Heyduk T and Heyduk E 2002 Molecular beacons for detecting DNA binding proteins *Nat. Biotechnol.* **20** 171–6
[33] Li J J, Fang X, Schuster S M and Tan W 2000 Molecular beacons: a novel approach to detect protein–DNA interactions *Angew. Chem.* **112** 1091–4
[34] Wu T-C, Biswas S, Dutta M and Stroscio M A 2011 Quantum-dot-based aptamer beacon for the detection of potassium ions *IEEE Trans. Nanotechnol.* **10** 991–5
[35] Wang Q, Chen L, Long Y, Tian H and Wu J 2013 Molecular beacons of xeno-nucleic acid for detecting nucleic acid *Theranostics* **3** 395–408
[36] Marras S A E, Tyagi S and Kramer F R 2006 Real-time assays with molecular beacons and other fluorescent nucleic acid hybridization probes *Clin. Chim. Acta* **363** 48–60
[37] Brenneman K L 2013 PhD Thesis *DNA-based Nanoconstructs for the Detection of Ions and Biomolecules with Related Raman/SERS Signature Studies* University of Illinois, Chicago
[38] Paroni R, Ceriotti F, Galanello R, Leoni G B, Panico A, Scurati E, Paleari R, Chemello L, Quaino V and Scaldaferri L 2007 Performance characteristics and clinical utility of an enzymatic method for the measurement of glycated albumin in plasma *Clin. Biochem.* **40** 1398–405
[39] Yamaguchi M, Kambe S, Eto T, Yamakoshi M, Kouzuma T and Suzuki N 2005 Point of care testing system via enzymatic method for the rapid, efficient assay of glycated albumin *Biosens. Bioelectron.* **21** 426–32
[40] Hatada M, Tsugawa W, Kamio E, Loew N, Klonoff D C and Sode K 2017 Development of a screen-printed carbon electrode based disposable enzyme sensor strip for the measurement of glycated albumin *Biosens. Bioelectron.* **88** 167–73
[41] Silver A C, Lamb E, Cattell W R and Dawnay A B S J 1991 Investigation and validation of the affinity chromatography method for measuring glycated albumin in serum and urine *Clin. Chim. Acta* **202** 11–22
[42] Yasukawa K, Abe F, Shida N, Koizumi Y, Uchida T, Noguchi K and Shima K 1992 High-performance affinity chromatography system for the rapid, efficient assay of glycated albumin *J. Chromatogr.* A **597** 271–5
[43] Rendell M, Rasbold K, Nierenberg J, Krohn R, Hermanson G, Klenk D and Smith P K 1986 Comparison and contrast of affinity chromatographic determinations of plasma glycated albumin and total glycated plasma protein *Clin. Biochem.* **19** 216–20
[44] Yamamoto Y, Tahara Y, Cha T, Noma Y, Fukuda M, Yamato E, Yoneda H, Hashimoto F, Ohboshi C and Hirota M 1989 Radioimmunoassay of glycated serum protein using monoclonal antibody to glucitollysine and coomassie-brilliant-blue-coated polystyrene beads *Diabetes Res.* **11** 45–9
[45] Ikeda K, Sakamoto Y, Kawasaki Y, Miyake T, Tanaka K, Urata T, Katayama Y, Ueda S and Horiuchi S 1998 Determination of glycated albumin by enzyme-linked boronate immunoassay (ELBIA) *Clin. Chem.* **44** 256–63
[46] Wilson R and Turner A P F 1992 Glucose oxidase: an ideal enzyme *Biosens. Bioelectron.* **7** 165–85
[47] Lehninger A L 1977 *Biochemistry* (New York: Worth Publishers)
[48] Fan Y, Tan X, Liu X, Ou X, Chen S and Wei S 2015 A novel non-enzymatic electrochemiluminescence sensor for the detection of glucose based on the competitive reaction between glucose and phenoxy dextran for concanavalin a binding sites *Electrochim. Acta* **180** 471–8
[49] Pandey R, Dingari N C, Spegazzini N, Dasari R R, Horowitz G L and Barman I 2015 Emerging trends in optical sensing of glycemic markers for diabetes monitoring *TrAC Trends Anal. Chem.* **64** 100–8
[50] Dingari N C, Horowitz G L, Kang J W, Dasari R R and Barman I 2012 Raman spectroscopy provides a powerful

diagnostic tool for accurate determination of albumin glycation *PLoS One* **7** e32406
[51] Kameya M, Tsugawa W, Yamada-Tajima M, Hatada M, Suzuki K, Sakaguchi-Mikami A, Ferri S, Klonoff D C and Sode K 2016 Electrochemical sensing system employing fructosamine 6-kinase enables glycated albumin measurement requiring no proteolytic digestion *Biotechnol. J.* **11** 797–804
[52] Kameya M, Sakaguchi-Mikami A, Ferri S, Tsugawa W and Sode K 2015 Advancing the development of glycated protein biosensing technology next-generation sensing molecules *J. Diabetes Sci. Technol.* **9** 183–91
[53] Inoue Y, Inoue M, Saito M, Yoshikawa H and Tamiya E 2017 Sensitive detection of glycated albumin in human serum albumin using electrochemiluminescence *Anal. Chem.* **89** 5909–15
[54] Fujii E, Shimizu K, Kurokawa Y K, Endo A, Sasaki S I, Kurihara K, Citterio D, Yamazaki H and Suzuki K 2003 Determination of glycosylated albumin using surface plasmon resonance sensor *Bunseki Kagaku* **52** 311–7
[55] Apiwat C, Luksirikul P, Kankla P, Pongprayoon P, Treerattrakoon K, Paiboonsukwong K, Fucharoen S, Dharakul T and Japrung D 2016 Graphene based aptasensor for glycated albumin in diabetes mellitus diagnosis and monitoring *Biosens. Bioelectron.* **82** 140–5
[56] Zuker M 2003 Mfold web server for nucleic acid folding and hybridization prediction *Nucleic Acids Res.* **31** 3406–15
[57] SantaLucia J 1998 A unified view of polymer, dumbbell, and oligonucleotide DNA nearest-neighbor thermodynamics *Proc. Natl Acad. Sci.* **95** 1460–5
[58] Peyret N 2000 PhD Thesis *Prediction of Nucleic Acid Hybridization: Parameters and Algorithms* Wayne State University, Detroit
[59] Arasteh A, Farahi S, Habibi-Rezaei M and Moosavi-Movahedi A A 2014 Glycated albumin: an overview of the *in vitro* models of an *in vivo* potential disease marker *J. Diabetes Metab. Disorders* **13** 49
[60] Luscombe N M, Laskowski R A and Thornton J M 2001 Amino acid–base interactions: a three-dimensional analysis of protein–DNA interactions at an atomic level *Nucleic Acids Res.* **29** 2860–74
[61] Kohzuma T, Yamamoto T, Uematsu Y, Shihabi Z K and Freedman B I 2011 Basic performance of an enzymatic method for glycated albumin and reference range determination *J. Diabetes Sci. Technol.* **5** 1455–62
[62] Testa R, Guerra E, Bonfigli A R, Di Gaetano N, Santini G and Ceriotti F 2016 Analytical performances of an enzymatic assay for the measurement of glycated albumin *J. Appl. Lab. Med. AACC Publ.* **1** 162–71
[63] Bunyarataphan S, Maruset L, Paiboonsukwong K, Fucharoen S, Dharakul T and Japrung D 2017 Glycated albumin detection using electrochemical aptasensor for screening and monitoring of diabetes mellitus *Meeting Abstracts* (Princeton, NJ: The Electrochemical Society) p 1956
[64] Kobayashi K, Yoshimoto K, Hirauchi K and Uchida K 1994 Determination of glycated proteins in biological samples based on colorimetry of 2-keto-glucose released with hydrazine *Biol. Pharm. Bull.* **17** 365–9
[65] PRD.7.ZQ5.10000007101 Product Specification